

**This document was prepared in conjunction with work accomplished under Contract No. DE-AC09-96SR18500 with the U. S. Department of Energy.**

**DISCLAIMER**

**This report was prepared as an account of work sponsored by an agency of the United States Government. Neither the United States Government nor any agency thereof, nor any of their employees, makes any warranty, express or implied, or assumes any legal liability or responsibility for the accuracy, completeness, or usefulness of any information, apparatus, product or process disclosed, or represents that its use would not infringe privately owned rights. Reference herein to any specific commercial product, process or service by trade name, trademark, manufacturer, or otherwise does not necessarily constitute or imply its endorsement, recommendation, or favoring by the United States Government or any agency thereof. The views and opinions of authors expressed herein do not necessarily state or reflect those of the United States Government or any agency thereof.**

**This report has been reproduced directly from the best available copy.**

**Available for sale to the public, in paper, from: U.S. Department of Commerce, National Technical Information Service, 5285 Port Royal Road, Springfield, VA 22161,  
phone: (800) 553-6847,  
fax: (703) 605-6900  
email: [orders@ntis.fedworld.gov](mailto:orders@ntis.fedworld.gov)  
online ordering: <http://www.ntis.gov/ordering.htm>**

**Available electronically at <http://www.doe.gov/bridge>  
Available for a processing fee to U.S. Department of Energy and its contractors, in paper, from: U.S. Department of Energy, Office of Scientific and Technical Information, P.O. Box 62, Oak Ridge, TN 37831-0062,  
phone: (865)576-8401,  
fax: (865)576-5728  
email: [reports@adonis.osti.gov](mailto:reports@adonis.osti.gov)**

WSRC-MS-99-00493

Kerry A. Dunn<sup>1</sup>, McIntyre R. Louthan, Jr.<sup>1</sup>, John I. Mickalonis<sup>1</sup>, Stuart Maloy<sup>2</sup>, Michael R. James<sup>2</sup>

## **Examination Of 304L Stainless Steel To 6061-T6 Aluminum Inertia Welded Transition Joints After Irradiation In A Spallation Neutron Spectrum**

---

Dunn, K. A., Louthan, M. R., Jr., Mickalonis, J. I., Maloy, S, James, M. R.,  
**“Examination Of Irradiated 304L Stainless Steel To 6061-T6 Aluminum Inertia Welded Transition Joints,”** *Effects of Radiation on Materials, ASTM STP 1405*, S. E. Rosinski, Eds., American Society for Testing and Materials, West Conshohocken, PA, 19428-2959

**Abstract:** The Savannah River Technology Center (SRTC) designed and fabricated tritium target/blanket assemblies which were irradiated for six months at the Los Alamos Neutron Science Center (LANSCE). Cooling water was supplied to the assemblies through 1 inch diameter 304L Stainless Steel (SS) tubing. To attach the 304L SS tubing to the modules a 304L SS to 6061-T6 Aluminum (Al) inertia welded transition joint was used. These SS/Al inertia weld transition joints simulate expected transition joints in the Accelerator Production of Tritium (APT) Target/Blanket where as many as a thousand SS/Al weld transition joints will be used. Materials compatibility between the 304L SS and the 6061-T6 Al in the spallation neutron environment is a major concern as well as the corrosion associated with the cooling water flowing through the piping. The irradiated inertia weld examination will be discussed.

**Keywords:** Corrosion, irradiation, inertia weld, weld, pitting, interface, galvanic corrosion, aluminum, stainless steel, spallation

### **Introduction**

The Accelerator Production of Tritium (APT) program is coordinated by Los Alamos National Laboratory (LANL) for the Department of Energy (DOE)/ Defense Programs (DP). The Savannah River Technology Center (SRTC) designed and fabricated tritium target/blanket assemblies which were sent to LANL and irradiated for six months at the Los Alamos Spallation Radiation Effects Facility (LASREF) at the Los Alamos Neutron Science Center (LANSCE). The cooling water was supplied to the assemblies through 1 inch diameter 304L stainless steel (SS) tubing. To attach the 304L SS tubing to the assemblies a 304L SS to 6061-T6 Aluminum (Al) inertia welded transition joint was used.

---

<sup>1</sup>Fellow, Sr. Advisory, and Principal Engineers, respectively, Westinghouse Savannah River Company, 773-41A, Aiken, SC 29808

<sup>2</sup>Materials Team Leader, Staff Member, respectively, Los Alamos National Laboratory, MS H809 APT-TPO, Los Alamos, NM 87545

Four SS/Al weld transition joints were attached to each Mark I and Mark II assembly (two inlet and two outlet cooling lines). In addition, two SS/Al weld transition joints (one inlet and one outlet) were attached to each of three High Flux Assemblies. Several thousand of these inertia welds are currently in the design for the APT Target/Blanket (T/B). In the APT design, aluminum piping in the target/blanket region houses the  $^3\text{He}/^3\text{H}$  gas. During production, this gas is transferred to the extraction and purification facility, where SS piping is used. The Al/SS inertia weld provides the path for gas flow between these two systems. Materials compatibility between the 304L SS and the 6061-T6 Al in the radiation environment is a major concern as well as the corrosion associated with the cooling water that will interact with the piping in the APT facility.

Examination of the interior of the cooling water piping irradiated at LANSCE indicates that the cooling water chemistry provides a noticeable influence on the corrosion of both the inertia weld and the parent material. The effect of radiation on the inertia weld and surrounding area is being evaluated against the cooling water effect. In addition, corrosion on the outside of the piping is being investigated. This exterior corrosion is accelerated by the presence of nitric acid, which was formed by the combination of radiolysis of air and water from other components leaking during the irradiation.

Results from analyses of the irradiated 304L to 6061-T6 Al inertia welds were obtained using a variety of methods including visual examination, microstructural analysis, hardness measurements, optical microscopy, Scanning Electron Microscopy (SEM), Energy Dispersive Spectroscopy (EDS) and electrochemical corrosion testing. All of the data gathered will be used to evaluate the concepts and methods for target/blanket manufacturing, materials and weld metal properties for spallation neutron environments, and joining methods for aluminum and aluminum to stainless steel.

## Experimental Design

Several prototypical target/blanket assemblies were fabricated for irradiation testing in the LANSCE facility at LANL. These target/blanket assemblies consisted of lead encapsulated in aluminum. The lead surrounded Al tubes filled with either helium-3 ( $^3\text{He}$ ) gas, or solid aluminum-lithium targets. The lead acted as a moderator and also provided an additional source of neutrons from n,xn spallation reactions. Cooling water was supplied to the target/blanket assemblies in the LANSCE facility via 1 inch diameter 304L stainless steel tubing. In order to transition from the 1 inch stainless steel cooling water tubing to the aluminum cooling water piping, a 304L stainless steel to 6061-T6 aluminum inertia welded transition joint was utilized [1]. The transition joint was machined from a commercial, inertia welded part made by Interface Welding [2]. Certification data sheets, supplied by the vendor, show that the solid state welds have a tensile strength equivalent to the 6061-T6 aluminum base metal in the T4 condition near the interface and a helium leak rate of approximately  $10^{-9}\text{cc}^3\text{He}/\text{sec}$ . The piping

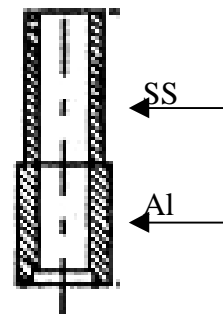


Figure 1. Detail of Inertia Welded Piping

details are shown in Figure 1 and the solid inertia welded piece prior to machining is shown in Figure 2.

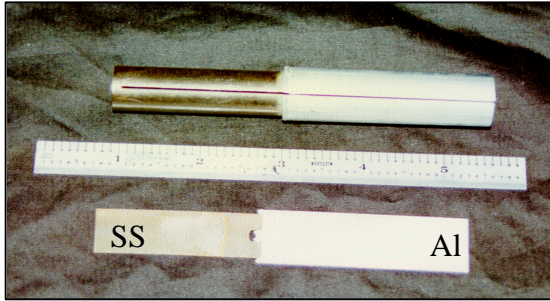
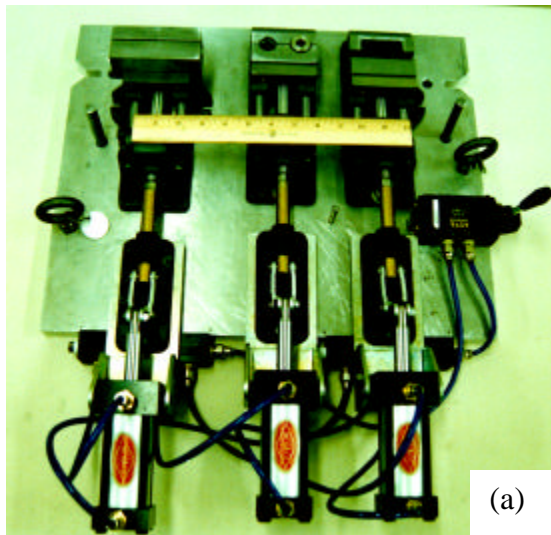


Figure 2. Solid Inertia Welded Piece Prior to Machining.

task plan outlined the deliberate and purposeful approach taken to accomplish the intended tasks.

A fixture and cutting apparatus was designed, fabricated and mocked up at SRS to support the sectioning of the irradiated inertia welded samples in the Chemical and Metallurgical Research (CMR) facility at LANL, Figure 3. The cutting apparatus was designed to provide ease of operation in the hot cells because of the difficulty working with manipulators. Clean inertia welded transition joints were used in the mock-up operation at SRS to ensure the cutting apparatus would operate smoothly in the hot cells. Once the mock-up operation at SRS was complete the cutting apparatus was transferred to the LANL CMR hot cells.



(a)



(b)

Figure 3. (a) Fixture used to section pieces in the hot cell. (b) Sectioned pieces.

Metallographic preparation equipment, which would be compatible with the hot cell environment, was purchased and mocked up at SRS prior to transfer to the LANL hot cells. Remote handling of the samples and the limited use of fluids in the hot cells needed to be considered for the operation. Several modifications to the equipment were made to make the equipment compatible with the hot cells. These modifications included the attachment of remote water lines to allow for the introduction of water from outside the hot cells and the displacement of the power operation to the exterior of the hot cells.

Once the modifications and mock-up were completed the equipment was transferred to the LANL hot cells.

## Experimental Setup

The prototypical lead/aluminum blanket assemblies were fabricated at the Savannah River Site (SRS) and transferred to LANL for introduction to Area A at the LANSCE facility. The assemblies were attached to the shielding inserts by welding the stainless steel water cooling lines to just above the transition joints as shown in Figure 4. The inserts were placed in a location downstream of the primary target inserts and outside of the direct proton beam. Over the course of the six-month irradiation, the Mark I and Mark II assemblies saw a neutron fluence of approximately  $8 \times 10^{19}$  n/cm<sup>2</sup>. The fluence from secondary protons was very small ( $< 3.0 \times 10^{18}$  p/cm<sup>2</sup>). The High Flux assemblies, located closer to the tungsten spallation target, saw approximately  $1 \times 10^{20}$  n/cm<sup>2</sup> with a negligible proton fluence. The cooling water used for this particular irradiation at LASREF was the X02 water source, which was a recirculating water system that cooled many areas of the irradiation including a copper beam stop. Thermocouples placed on the outside of the cooling lines indicated that the temperatures in the location where the Mark I and Mark II as well as the high flux assemblies were maintained at approximately 30°C.

Following irradiation, the assemblies were detached from the shielding inserts and transferred in a cask from LASREF to the CMR facility at LANL where they were placed in the hot cells in Wing 9. The inertia welded sections, separated from the assemblies prior to movement to the CMR facility, were then removed from the transfer cask and placed in the Wing 9 hot cell facility.

The fixture and cutting apparatus was used to separate the sleeve from the transition joints prior to sectioning the samples for further examination. Once the sleeve was removed the inertia welded transition joints were placed in the fixtures and sectioned in half and then one of the cut pieces was sectioned in half again, creating two  $\frac{1}{4}$  sections and one  $\frac{1}{2}$  section. After visual examination, a  $\frac{1}{4}$  section of each transition joint was mounted for metallographic preparation. The remaining two pieces were available for additional testing such as SEM/EDS or x-ray analysis.

Metallographic equipment was introduced to the hot cells. Steps necessary for properly preparing the irradiated samples were developed at SRS and those techniques were transferred to LANL. Because of the dissimilar metals at the weld interface,

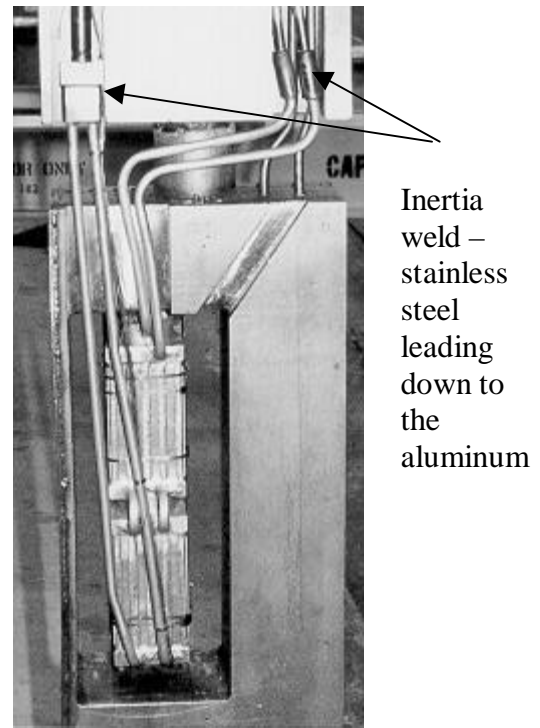


Figure 4. Inertia welded transition joints welded to cooling water piping.

metallographic preparation of these specimens was not straightforward. Rounding of the aluminum edges was a great concern because Al is a softer material than stainless steel. However, metallographic preparation of the specimen using standard techniques for aluminum samples would not ensure that the stainless steel microstructure would be properly prepared for examination. An added intricacy was the fact that this metallographic preparation would take place in the hot cells at LANL where manipulators would be used and a minimum amount of liquids was allowed. As a result of several iterations with the non-irradiated inertia welded samples and the mock-up operation at SRS, a metallographic technique was developed that provided the optimum operating parameters to ensure a properly prepared sample (Table 1 and Table 2). A baseline characterization of non-irradiated Al-SS inertia welded transition joints was completed to support the characterization of the irradiated transition joints [4].

A sample from each inertia welded transition joint was mounted and prepared metallographically. In addition, a non-irradiated inertia welded transition joint (control sample) was prepared metallographically in the hot cells to compare to the irradiated specimens.

**Table 1** – Sample preparation sequence for metallographic analysis using automated grinder/polisher.

<b>Grinding/Polishing Sequence</b>	<b>Preparation Time (seconds)</b>	<b>Application Force (N)</b>
500, 600, 800, 1200, 2400 grit SiC Papers	90 (Each)	100,150,100 (Each)
1 μm Diamond Nap Cloth	240	200, 150, 100
6 μm Diamond Nap Cloth	240	200,150,100

Note: Application forces vary among the three listed for each preparation step.

**Table 2** – Exposure times and compositions of etchants used in metallographic analysis.

<b>Poulton's Etching Solution (Al etchant)</b>	<b>Oxalic Acid Solution (SS etchant)</b>
50 mL Poulton's Reagent <sup>1</sup> 40 mL chromic acid solution <sup>2</sup> 25 mL HNO <sub>3</sub>	10 g oxalic acid 100 mL H <sub>2</sub> O (6V applied to solution)
<u>Exposure Time: 10 sec.</u>	<u>Exposure Time: 60 sec.</u>

<sup>1</sup>12 parts HCl, 6 parts HNO<sub>3</sub>, 1 part HF, 1 part H<sub>2</sub>O

<sup>2</sup>3 g chromic acid per 10 mL H<sub>2</sub>O

Electrochemical corrosion tests were performed to evaluate the corrosion process at the weld interface as a function of water chemistry. The galvanic interactions between aluminum and stainless steel were suspect. The corrosion tests included potential and galvanic current monitoring and potentiodynamic polarization. Samples for electrochemical testing were obtained from the same as-received inertia welded slugs that

were used for the irradiated sections. Additional test samples included the Al parent metal, the stainless steel parent metal, and the Heat Affected Zone (HAZ) of the Al. The samples were prepared as metallographic mounts with electrical connections for the electrochemical tests.

The water chemistries were simulated conditions for X02 water, dirty APT water and APT water. For the simulated APT water, laboratory distilled water was used since the impurity levels were low and similar to that anticipated for the APT. The dirty APT water had 2 ppm  $\text{Cl}^-$  and 7 ppm  $\text{SO}_4^-$ . The X02 water was a derivative of the dirty APT water with added copper, either 1.0 ppm Cu (XO2b) or 0.1 ppm Cu (XO2a). All the waters were adjusted to a pH 5 with nitric acid and had hydrogen peroxide levels of 0.001 M.

Testing was conducted in a blackened glass cell equipped with gas spargers. When deaerating, nitrogen gas was used. A Ag/AgCl electrode was used as the potential reference and graphite rods were the counter electrodes. A standard laboratory stir/hot plate was used for agitation and heating. All tests were conducted at 30° C.

## Experimental Results and Discussion

### Corrosion

Over the course of the irradiation, some leaks developed, from other components in Area A, which produced a spray of the cooling water to the exterior of the target/blanket assemblies. Radiolysis of this water in the air environment created a nitric acid spray on the components in Area A. Corrosion on the outside of the assemblies was clearly evident following irradiation and has been attributed, primarily, to the presence of the nitric acid, Figure 5.

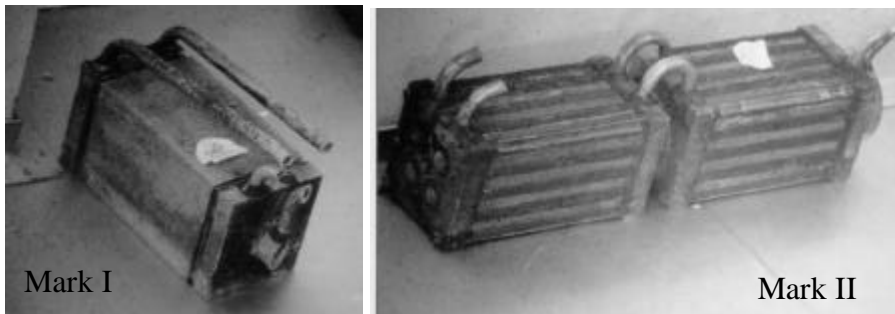


Figure 5. Mark I and Mark II following irradiation showing corrosion product.

Visual examination of the sectioned inertia welded transition joints showed the presence of corrosion on not only the exterior of the cooling water tubing but also on the interior of the tubing. The corrosion was evident both on the aluminum section of the cooling water tubing and at the inertia welded interface, Figures 6-7. The stainless steel was relatively unaffected. Differences in the appearance of the corrosion on the aluminum metal and at the inertia welded interface was clearly evident between the different samples.

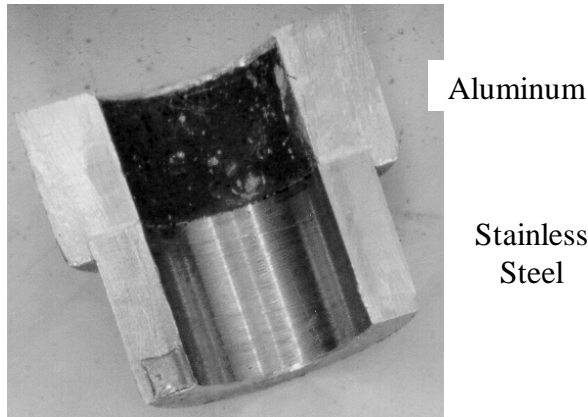


Figure 6. Inside wall of cooling line from Mark II assembly. Note black corrosion product on aluminum.

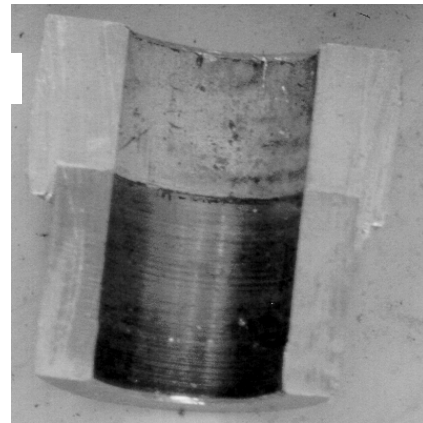


Figure 7. Inside wall of cooling line from High Flux Assembly. Note the greyish oxide on aluminum.

### *Metallographic Examination*

Samples from each assembly (Mark I, Mark II and High Flux Assemblies) were sectioned, prepared metallographically and examined in CMR hot cells. Because Al and SS are dissimilar metals, the inertia welded interface is susceptible to galvanic corrosion. Metallographic examination of the irradiated inertia welds indicates that some of the samples did exhibit degradation at the interface, which is characteristic of galvanic corrosion, Figure 8. However, general corrosion along the length of the aluminum piping

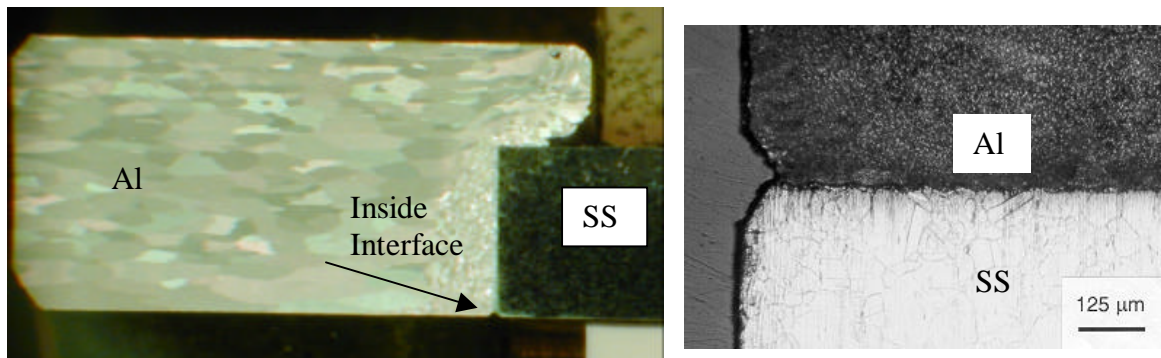


Figure 8. Slight degradation at inertia welded interface on the cooling water side of the High Flux inlet piece (a) macrograph and (b) higher magnification of inside at interface.

and pitting corrosion were more prevalent, Figure 9. The pitting corrosion appeared to present the most severe effects of corrosion. This pitting corrosion, which is located along the piping away from the interface, indicates that the effect of the cooling water chemistry, flow rate and irradiation all need to be scrutinized more than the effect of corrosion due to the galvanic couple at the stainless steel to aluminum weld interface.

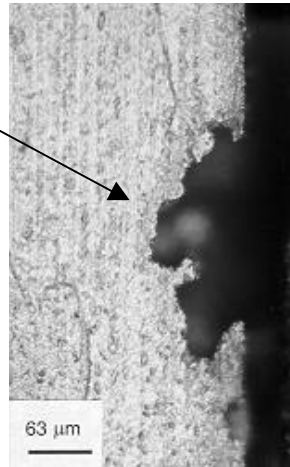
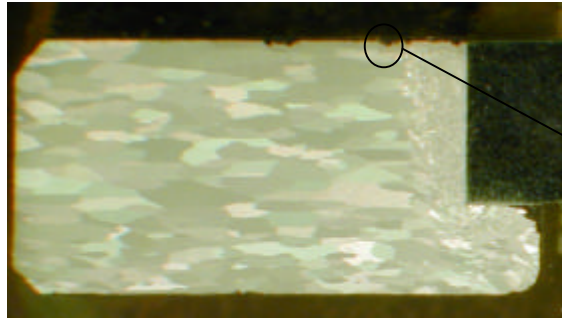


Figure 9. Pitting corrosion along the length of the aluminum on the cooling water side of the Mark I outlet piece (a) macrograph and (b) higher magnification of inside aluminum wall showing representative pitting.

The cooling water used for the Mark I, Mark II and high flux assemblies was provided from the XO2 system. This XO2 system contains more contaminants than are

expected in the APT

facility where the water chemistry will be more stringently controlled.

Flow of the XO2 cooling water through the 9A and 9C inserts (Mark II and Mark I) was 7.5 and 7.0 gpm, respectively, while the flow through the 18B insert (high flux assemblies) was 25.86 gpm. As a result of these different cooling water flow rates, oxide thickness on the inside wall of the cooling water piping from the 9A and 9C inserts was approximately 50 μm while the oxide layer on the cooling water piping from the 18B

insert was approximately 15 μm, Figure 10.

Because the temperature of the cooling water was maintained at approximately 30°C the predominant oxide layer was Bayerite, ( $\beta$ - $\text{Al}_2\text{O}_3 \cdot 3\text{H}_2\text{O}$ ).

Initially, Gibbsite ( $\alpha$ - $\text{Al}_2\text{O}_3 \cdot 3\text{H}_2\text{O}$ ) is formed before a phase change to

Bayerite [5]. Fifty μm is the maximum oxide thickness expected for the Area-A test conditions [6].

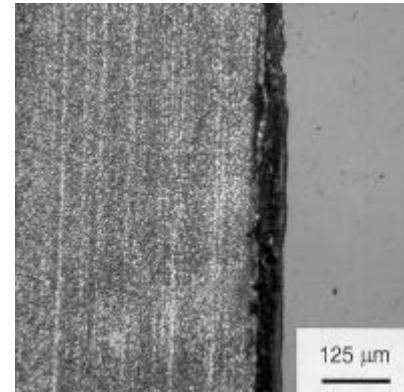
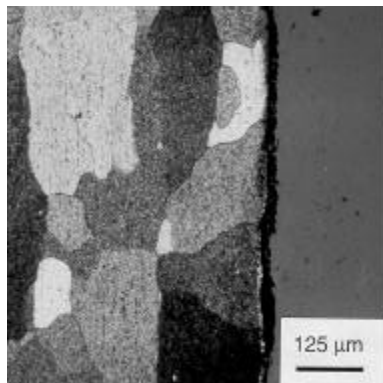


Figure 10. Oxide buildup on inside wall of aluminum cooling water piping near the inertia weld (a) high flux section (25.86 gpm) (b) Mark I section (7.0gpm).

Another observation made during the metallographic examination is the effect of recrystallization of the Heat Affected Zone (HAZ) in the aluminum at the inertia welded interface and grain growth in the aluminum parent material. In each of the unirradiated inertia welded samples prepared for the baseline study, as well as the control sample that was prepared in the CMR hot cells, the HAZ does not show the presence of individual grains in the structure, Figure 11. In addition, the grain structure in the Al parent material of the unirradiated samples shows small equiaxed grains along the outside of the samples

with an elongated grain structure near the inside of the samples, Figure 12. However, all of the irradiated inertia welded samples show grain definition in the heat affected zone of the aluminum, indicating recrystallization, and grain growth in the Al parent material, Figure 9(a), 10(a) and 13. The grain growth in the parent material resulted in a fairly consistent grain size throughout the microstructure. Because of the low dose these samples received and the low temperatures measured during irradiation, 30°C, the only



Figure 11. Control sample metallographically prepared in CMR hot cells. Solid inertia welded piece machined to simulate irradiated sections.

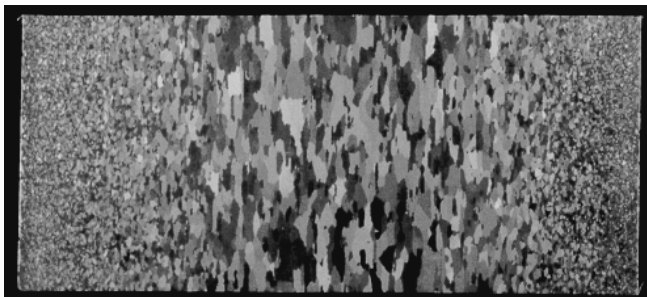


Figure 12. Grain size variation across solid aluminum parent metal from inertia welded specimens.

explanation for the recrystallization and grain growth is that these specimens were heated during welding before irradiation. Hardness measurements were performed on the inertia welded non-irradiated as well as the irradiated samples to evaluate differences as a result of the recrystallization and grain growth. Hardness values in the non-irradiated samples were higher than those in the irradiated samples, as shown in Figure 14. These hardness results indicate an aged structure in the irradiated samples and, hence, a reduction in strength. This reduction in strength did not present any deleterious effects during the six month irradiation. However, it is a consideration in the APT design and proper cooling techniques must be employed when joining the 6061-T6 aluminum tubing associated with the inertia weld to the aluminum tubing in the target/blanket region of the APT facility. The mechanical properties of inertia welded tensile specimens did not degrade during the irradiation [7].

The temperature typically used to induce this type of behavior is approximately 415°C for a 2-3 hour

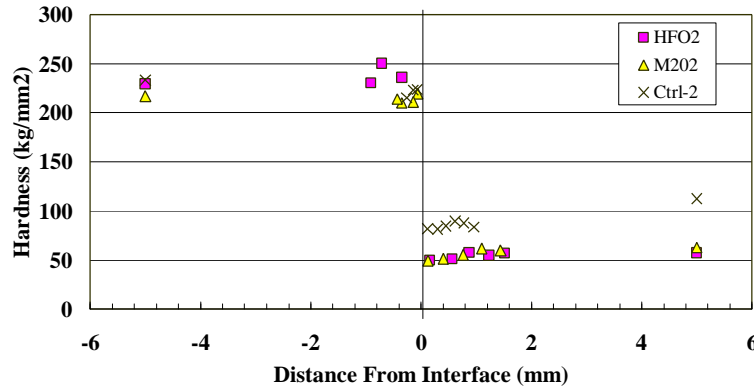
explanation for the recrystallization and grain growth is that these specimens were heated during welding before irradiation. Hardness measurements were performed on the inertia welded non-irradiated as well as the irradiated samples to evaluate differences as a result of the recrystallization and grain growth. Hardness values in the non-irradiated samples were higher than those in the irradiated samples, as shown in Figure 14. These hardness results indicate an aged structure in the irradiated



Figure 13. Irradiated piping from High Flux outlet section showing evidence of recrystallization at inertia welded interface (HAZ) and grain growth across the Al parent metal.

period of time [8]. An inertia welded sample was sectioned into quarters for evaluating the effect of temperature on the recrystallization and grain growth of the HAZ and Al material. One quarter section was heated at 200°C and a second quarter section was heated at 300°C, each for a 24 hour period. No recrystallization or grain growth was observed in these test samples.

**Figure 14. Hardness vs. Position for Stainless Steel/Aluminum Inertia Welds**



**Scanning Electron Microscopy and Energy Dispersive Analysis**

The primary focus of the SEM and EDS study was to investigate the interior of the inertia welded specimens. The exterior of the piping of the samples generally indicated corrosion product consistent with an aluminum oxide, Figure 15. The interior of the

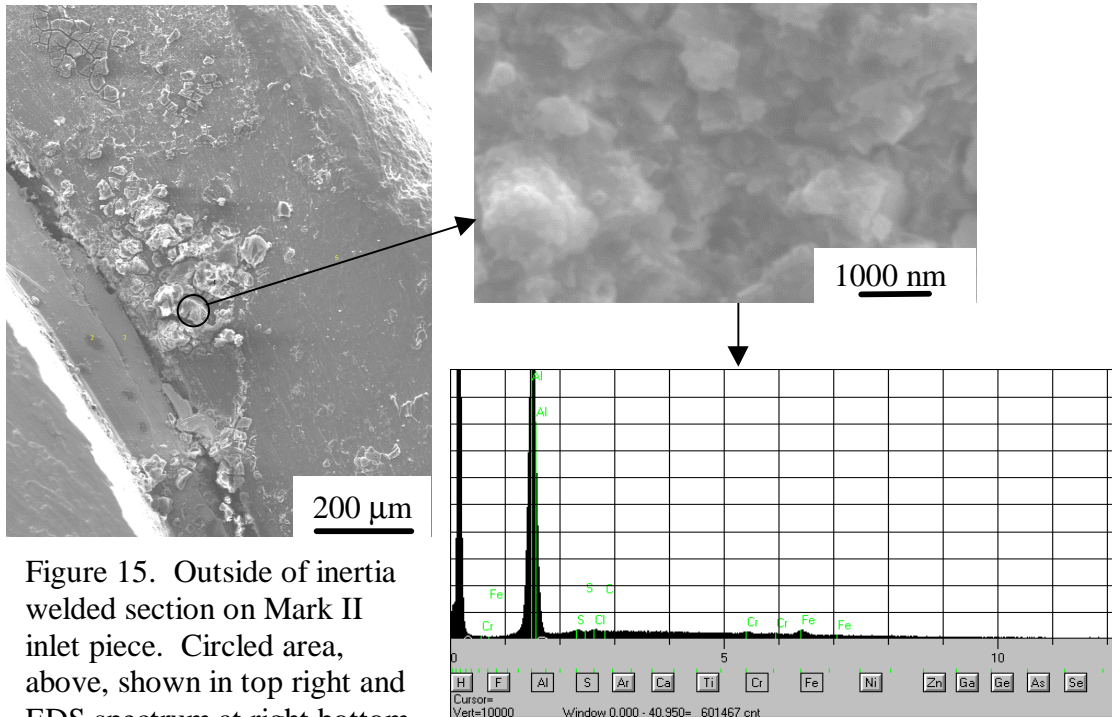


Figure 15. Outside of inertia welded section on Mark II inlet piece. Circled area, above, shown in top right and EDS spectrum at right bottom indicates aluminum oxide.

inertia welded specimens showed a high degree of oxidation on the aluminum portion of the specimens, Figure 16, consistent with the previous visual examinations.

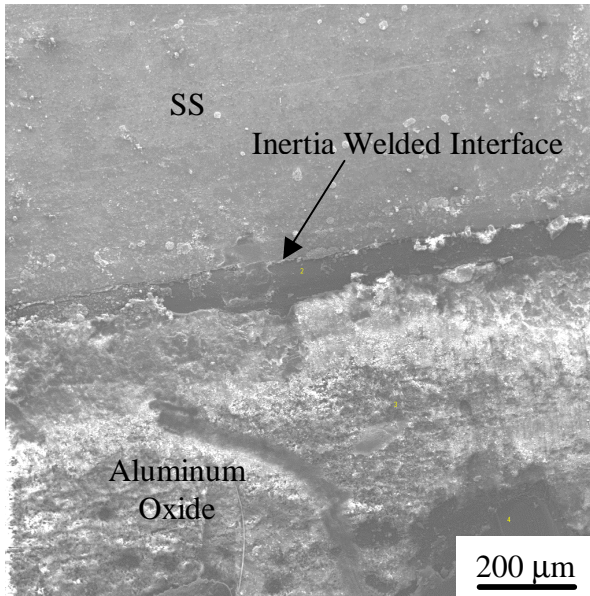


Figure 16. SEM of inside weld taken from High Flux Assembly on inertia welded interface. Note the region of “flaked-off” corrosion product adjacent to the interface.

Several areas observed had portions of the aluminum oxide that had flaked off of the surface, exposing another layer below the outer layer, Figure 16, which is consistent with earlier findings. The presence of a “mud-flat cracking” appearance was evident on several samples, Figure 17. This flaking of the oxide layer and “mud-flat cracking” is consistent with the presence of  $Al_2O_3 \cdot 3H_2O$ , which does not adhere well to the surface of the aluminum substrate.

Flow rate of the three assemblies placed in the Area A irradiation were different. Flow of the  $XO_2$  cooling water through the 9A and 9C inserts (Mark I and Mark II) was 7.5 and 7.0 gpm, respectively, while the flow through the 18B insert (High Flux assemblies) was 25.86 gpm. The oxide layer adjacent to

the weld interface shown in Figure 16 and 17 (High Flux) has flaked off while the oxide layer shown in Figure 18 (Mark II) does not indicate flaking. This observation is consistent with the increased agitation from the flow rate with the High Flux assemblies

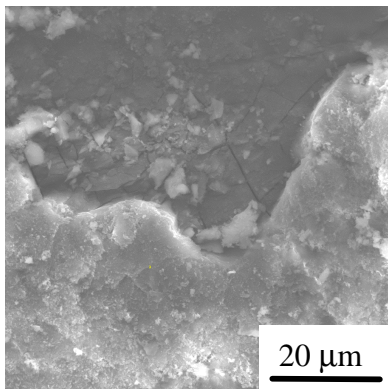


Figure 17. Mudflat cracking of oxide layer in High Flux sample.

and the observation made visually and with metallography, Figures 6, 7 and 10.

Another observation with the SEM was the presence of copper (Cu) rich deposits on the surface of the stainless steel, Figure 19. No evidence of the copper deposits was seen on the aluminum material.

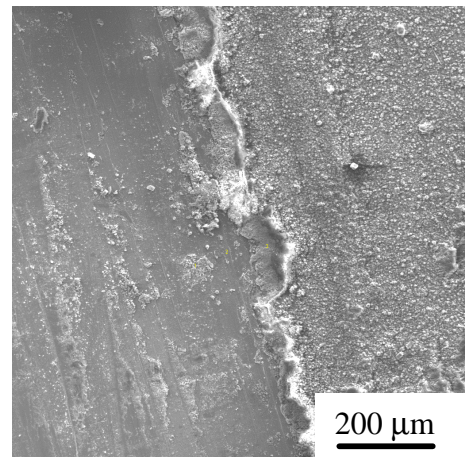


Figure 18. SS/Al interface of Mark II with Al oxide adhering to the surface.

However, the  $Al_2O_3 \cdot 3H_2O$  oxide layer was fairly thick and masked the presence of the copper deposits. Copper deposits on aluminum are known to cause pitting, which would explain

the pitting corrosion observed in the metallographic specimens, Figure 9. The copper deposits were present as a result of the corrosion of the copper beam stop, which was also cooled by the XO2 cooling water system.

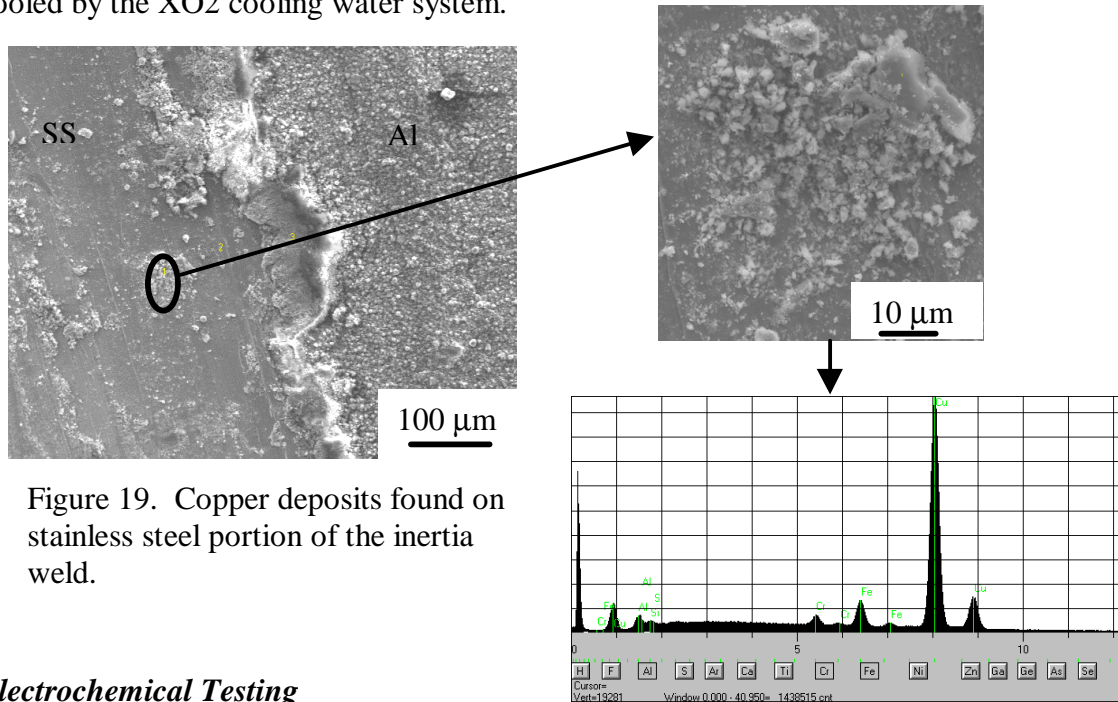


Figure 19. Copper deposits found on stainless steel portion of the inertia weld.

### ***Electrochemical Testing***

Corrosion processes characterized through the electrochemical testing were found to be consistent with those observed on the irradiated inertia welds from the Mark I, Mark II, and high flux assemblies. Galvanic and pitting corrosion were the primary mechanisms, similar to the irradiated inertia welds. These processes were more aggressive in the water chemistries with higher impurities. XO2 water chemistries produced the most significant pitting and the highest galvanic currents. The test results are summarized in Table X, which gives the nominal galvanic current of the stainless steel/aluminum couple and open-circuit potentials.

Open-circuit potential measurements were made on samples of the parent material as well as a section of the weld. As expected, 304L stainless steel was more electropositive than aluminum. The potential of the weld fell between that of the two parent materials. The potential of aluminum was variable for a given water due to the oxide formation dependence on water chemistry. The presence of copper in the XO2 water chemistry caused the potential of both stainless steel and aluminum to shift to more electropositive values. This shift was attributed to the increase in the cathodic reaction due to the reduction of copper.

As the impurity level of the water increased the galvanic current increased. This large galvanic interaction lead to more significant pitting on the aluminum samples. The worst pitting was observed in the XO2 waters. In the XO2 waters, the high degree of pitting was associated with the deposition of copper. The stainless steel sample had the most deposits. Some pitting was also observed on the stainless steel in the XO2b water. These pits were associated with copper deposits on the surface. Few copper deposits were observed on the aluminum sample. The results show that 304L stainless steel is the

cathode in the couple where the reduction of copper occurs. These results are consistent with those observed on the irradiated inertia welds.

**Table 3 - Galvanic Current and Potential Measurements**

<b>Water Test Solution</b>	<b>Galvanic Current</b>	<b>Aluminum potential</b>	<b>Stainless steel potential</b>	<b>Weld potential</b>
<b>Typical APT</b>	0.75	-0.375	0.375	-0.290
<b>Dirty APT</b>	5.5	-0.250	0.330	-0.23
<b>XO2a</b>	7	-0.225	0.400	ND
<b>XO2b</b>	8.75	0.250	0.410	ND

### Summary

No leaking at the inertia welded interface was observed following irradiation. The galvanic interaction at the 6061 Al to 304L stainless steel inertia welded interface did not present significant degradation as a result of the irradiation or the cooling water chemistry. General corrosion was evident along the entire length of the aluminum piping. Pitting corrosion was present along the aluminum piping and is attributed to conductivity of and copper deposits in the cooling water.

Water chemistry and flow rate are important considerations for the APT design. The reduction or elimination of impurities in the cooling water aids in corrosion control of the aluminum piping and the inertia welded interface. Static or low flow rate of cooling water provides an avenue for oxide buildup on the aluminum portion of the inertia weld while a higher flow rate induces flaking of the aluminum oxide layer.

Welding of these inertia welded sections to the aluminum cooling water piping caused recrystallization at the aluminum HAZ and grain growth in the parent material. This recrystallization and grain growth in the Al material resulted in a reduction in hardness of the aluminum material. Quality control of the welding procedures for the design and construction of the APT facility will have to be controlled via procedures that outline appropriate cooling mechanisms for the inertia welds.

### References

- [1] Peacock, Jr., H. B., and Leader, D. R., "Design and Fabrication of Prototypical APT Target/Blanket Assemblies and Weld Samples for Area-A Test in the LANSCE Facility at LANL", Internal Report WSRC-TR-96-0180, Westinghouse Savannah River Company, Aiken, SC, April, 1997.
- [2] Wadleigh, Al S., "Bi-Metal Welding of Aluminum", Interface Welding, Carson, CA 90746
- [3] Dunn, K. A., "Task Technical Plan for Target/Blanket Materials Examination", Internal Report WSRC-RP-98-00038, Westinghouse Savannah River Company, Aiken, SC, May 7, 1998

- [4] Dunn, K. A., Tosten, M. H., Louthan, Jr., M. R., Birt, M. L., “Microstructural Characterization of 6061 Aluminum to 304L Stainless Steel Inertia Welds”, *Conference Proceedings from the 32<sup>nd</sup> Annual Convention of the International Metallographic Society (Understanding Processing/Structure/Property/Behavior)*, November, 1999.
- [5] Chandler, G. T., Sindelar, R. L., Lam, P. S., “Evaluation of Water Chemistry on the Pitting Susceptibility of Aluminum”, *Corrosion 97, Paper No. 104*, 1997.
- [6] Peacock, Jr., H. B., Sindelar, R. L., Lam, P. S., Murphy, T. H., “Evaluation of Corrosion of Aluminum Base Reactor Fuel Cladding Materials During Dry Storage” Internal Report WSRC-TR-95-0345, Westinghouse Savannah River Company, Aiken, SC, November 1995.
- [7] Louthan, M. R., Jr., et al, “Tensile Properties of Welded Alloy 718, 316L and 304L Stainless Steel and 6061 and 5052 Aluminum After Irradiation at the LANSCE Accelerator, To Be Published in ANS Journal.
- [8] “Heat Treating of Aluminum Alloys”, *Metals Handbook, Ninth Edition, Volume 2. Properties and Selection: Nonferrous Alloys and Pure Metals*, 1979, pp. 675-718.